Energy Advances

ROYAL SOCIETY OF CHEMISTRY

COMMUNICATION

View Article Online
View Journal | View Issue

Open Access Article. Published on 17 April 2023. Downloaded on 10/20/2025 5:22:59 PM.
This article is licensed under a Creative Commons Attribution-NonCommercial 3.0 Unported Licence.

Check for updates

Cite this: *Energy Adv.*, 2023, 2, 784

Received 4th March 2023,
Accepted 16th April 2023

DOI: 10.1039/d3ya00100h

rsc.li/energy-advances

Well-defined 2D transition vanadium pentoxide (V_2O_5) flat nanorods with large-scale synthesis feasibility as an electrocatalyst for the oxygen evolution reaction (OER)†

Veena Mounasamy, Ganesan Srividhya and Nagamony Ponpandian *

The unwavering focus on renewable energy generation has opened a wider research scope towards the study of electrocatalytic water splitting. In this regard, the present work deals with a low-cost synthesis strategy enabling large scale production of vanadium pentoxide (V_2O_5) electrocatalysts for the oxygen evolution reaction (OER). Polycrystalline V_2O_5 nanostructures with a 2D flat nanorod-like morphology with a rod length of about 1 μm were developed using a polymer-assisted solution technique. Benefitting from their unique morphology, V_2O_5 nanorods showed commendable OER properties with a low Tafel slope value of 88 mV dec^{-1} and overpotential (ηOER) of 310 mV at 10 mA cm^{-2}. With a stable catalytic performance for 12 h, the V_2O_5 nanorods grown with polymer assistance is proposed as a promising candidate for OER activity in the present study.

Introduction

Demand for sustainable energy as a fossil fuel alternative to tackle the global energy and environmental crisis has been driving attention towards electrocatalytic research over the past few decades. Among various evolution and reduction mechanisms involved in water splitting, the anodic oxygen evolution reaction is considered as a bottleneck in electrochemical water splitting applications.[1,2] To be an ideal electrocatalyst suitable for large scale production, the material must possess better catalytic activity, enhanced electrochemical surface area, cyclic stability, low toxicity and abundant availability. To date, ruthenium oxide (RuO_2) and iridium oxide (IrO_2) are widely studied for their OER behaviour.[3] Considering their limitations with respect to their cost and availability, it is believed that the transition metal oxides will be a promising alternative. Owing to its catalytic efficiency and activity at a wider pH range with technologically relevant factors in addition to availability, cost effectiveness and low toxicity, vanadium oxide (VO_x) has been chosen as an electrocatalyst in this work. The present work is focussed on a scalable synthesis strategy suitable for real time employability. The OER studies of transition metal oxides, specifically pure vanadium oxide (V_2O_5), a highly stable phase of vanadium oxide,[4] are very limited in the literature. As complicated synthesis procedures hamper scalability and repeatability, we believe that this work will be a prelude in diminishing those limitations and encourage further studies on OER behaviour of V_2O_5 nanostructures that can contribute much more to efficient water splitting.

Materials and methods

With a view to overcome rigorous procedures involved in developing metal oxide nanostructures, this work reports a low-cost synthesis procedure to develop V_2O_5 nanostructures using a polymer-assisted solution technique. This technique is simple, cost-effective and avoids complex procedures. In this work, 0.508 g of ammonium metavanadate (NH_4VO_3) and 2 g of poly vinyl alcohol (PVA) were dissolved in water at 80 °C and stirred (@500 rpm) for 72 hours. 3 drops of acetic acid were added to the above solution to attain suitable pH conditions. On long-term stirring, a highly viscous solution was formed. The solution was then transferred to a Petri dish and dried at 80 °C for 24 h. After drying, to completely oxidize and remove the polymer residues, the dried sample was annealed at 500 °C for 3 h (Fig. 1). The obtained VO_x samples were characterized by X-ray diffraction (XRD – Rigaku Ultima-III) with CuKα radiation and X-ray photoelectron spectroscopy (XPS – Quantum 2000, Physical Electronics, Inc., USA) for structural and compositional analysis and field-emission scanning electron microscopy (FESEM – JEOL, JCM 6000, Japan) for morphological analysis. The working electrode

Department of Nanoscience and Technology, Bharathiar University, Coimbatore 641046, India. E-mail: Ponpandian@buc.edu.in; Tel: +91-422-2428421

† Electronic supplementary information (ESI) available. See DOI: https://doi.org/10.1039/d3ya00100h

© 2023 The Author(s). Published by the Royal Society of Chemistry

Open Access Article. Published on 17 April 2023. Downloaded on 10/20/2025 5:22:59 PM.
This article is licensed under a Creative Commons Attribution-NonCommercial 3.0 Unported Licence.

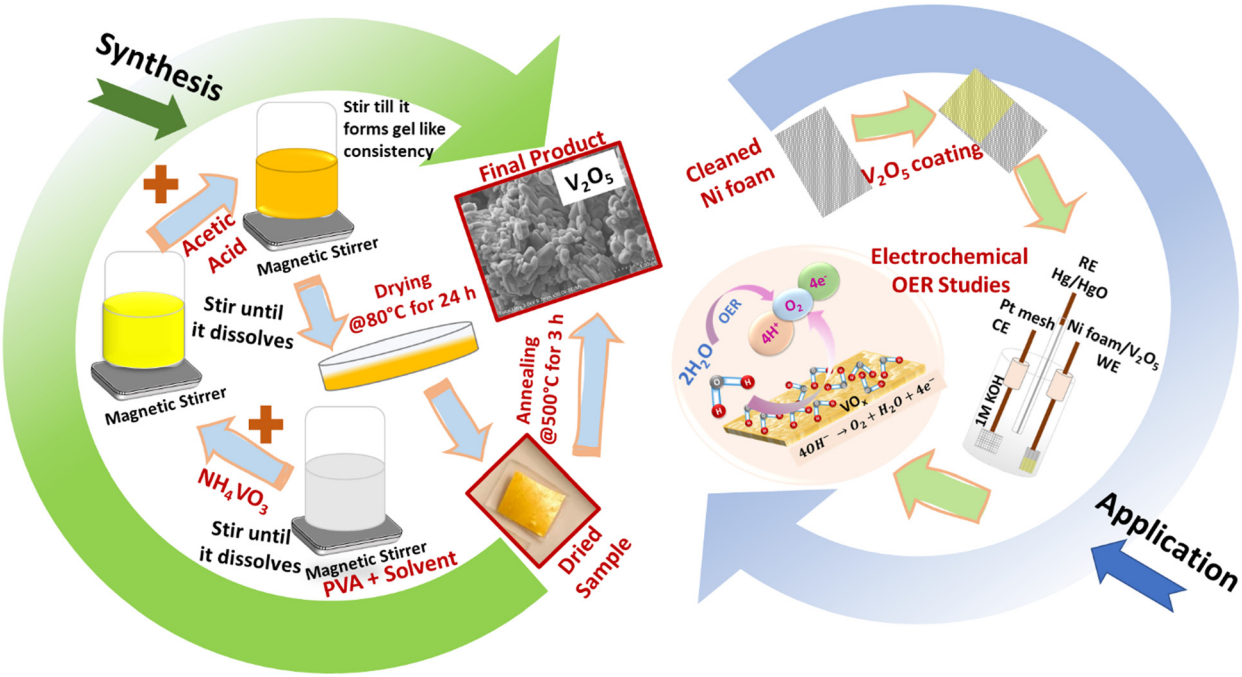

Fig. 1 Schematic representation of the V_2O_5 synthesis and its OER experiment.

was prepared by mixing V_2O_5 into a slurry with carbon black and PVDF in a 8 : 1 : 1 ratio and coated on nickel foam (NF) having (1 × 1 cm^2) dimension and allowed to dry @ 60 °C for 6 h. The studies were performed in 1 M KOH electrolyte, where platinum mesh (Pt) and Hg/HgO were used as counter and reference electrodes, respectively.

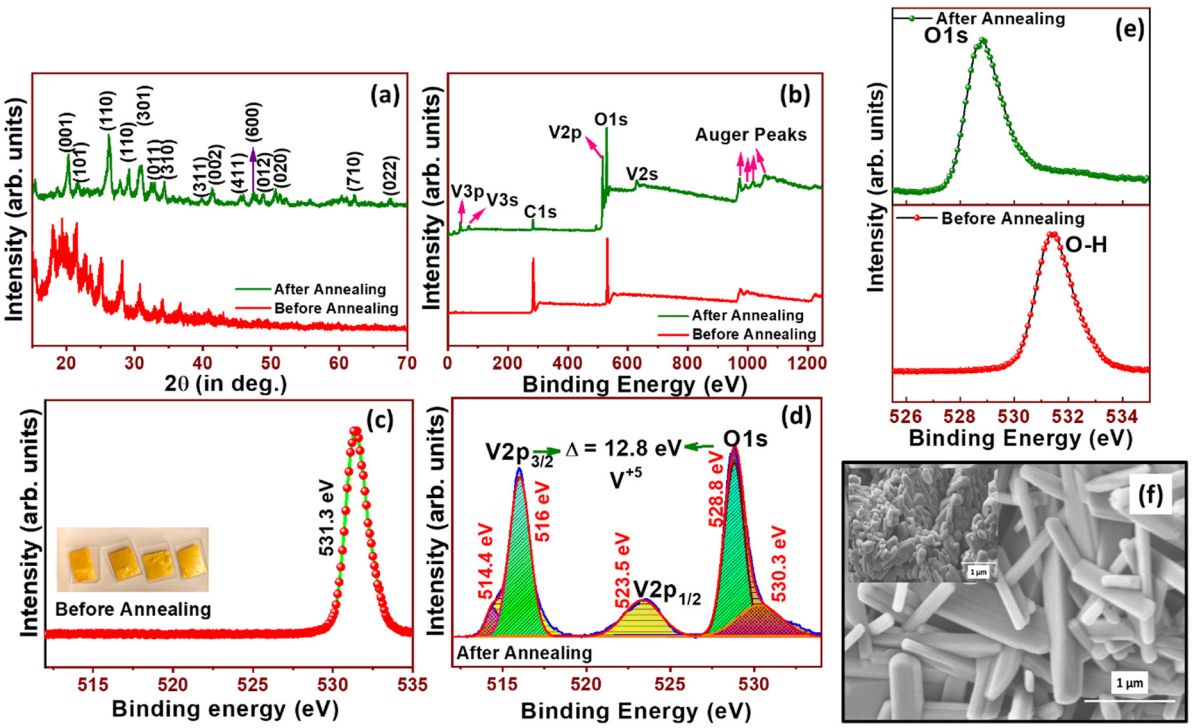

Fig. 2 (a) XRD spectra and (b) XPS survey spectra before annealing and after annealing, high resolution XPS spectra of (c) VO_x before annealing (inset: low magnification image) and (d) V_2O_5 after annealing, (e) O1s peaks, and FESEM image of (f) V_2O_5 flat nanorods.

Open Access Article. Published on 17 April 2023. Downloaded on 10/20/2025 5:22:59 PM.
This article is licensed under a Creative Commons Attribution-NonCommercial 3.0 Unported Licence.

Results and discussion

Fig. 2(a) shows the XRD spectra of VO_x nanoparticles before and after annealing. Before annealing, vanadium was not completely oxidized and hence the wider peaks were observed in the XRD spectrum. After annealing, well-defined peaks were observed. The 2θ peaks at 20.3°, 21.7°, 26.2°, 30.9°, 32.3°, 34.3°, 39.8°, 41.4°, 45.9°, 50.7°, 47.4°, 48.8°, 62.1° and 67.5° confirmed the presence of polycrystalline orthorhombic V_2O_5 (ICDD card no. 00-041-1426) phase. From the XRD spectrum, it is seen that V_2O_5 is completely in the V_2O_5 phase without any mixed phases. VO_x is a highly challenging material in determining its phase, as its oxidation state is widely spread between V^{3+} and V^{5+}. In spite of several oxide phases of vanadium, V_2O_5 is the stable phase of vanadium and highly suitable for catalytic activities. Fig. 2(b) shows the survey spectra of VO_x before and after annealing. Due to the incomplete phase formation before annealing, there are no vanadium peaks in the narrow spectra (Fig. 2(c)). In the high resolution XPS narrow spectrum shown in Fig. 2(d), related to the annealed sample, the peaks at 516 and 523.5 eV corresponding to $V2p_{3/2}$ and $V2p_{1/2}$ respectively and peak at 528.8 eV corresponding to the O1s peak confirmed the V^{+5} oxidation state. The peak difference between $V2p_{3/2}$ and O1s (Δ eV) is 12.8 eV, which also confirmed the V^{+5} oxidation state. Fig. 2(e) also reveals that there are chances of OH adsorbed on vanadium (V) from its double peak corresponding to oxygen.[5] The shift in oxygen peak as a result of annealing was also noticed. With regard to the morphology of the synthesized V_2O_5 nanostructures, from Fig. 2(f), flat nanorod-like 2D structures of V_2O_5 with fewer voids were noticed. As the synthesis procedure involved the inclusion of PVA, during the annealing process at high temperature for oxidation *i.e.*, 500 °C for 3 h, the PVA was decomposed/removed making voids in the morphology as indicated in ESI† S1. The nanorod-like structures with ~1 μm length will be helpful in enhancing the electrochemical activity towards OER studies due to their increased surface area and well-defined morphology. The linear sweep voltammetry (LSV) polarization curves recorded at 5 mV s^{-1} for bare Ni foam (NF) and NF/V_2O_5 are presented in Fig. 3(a), where NF/V_2O_5 shows a substantially low overpotential (η) of 310 mV, when compared to bare NF with 410 mV at a current density of 10 mA cm^{-2}. To comprehend the intrinsic catalytic activity of the prepared catalyst, Tafel analysis was carried out from LSV study and the plots are represented in Fig. 3(b). It can be seen that NF shows a Tafel slope value of 268 mV s^{-1}, whereas NF/V_2O_5 shows a lower Tafel slope of 88 mV dec^{-1}, which suggests that V_2O_5 facilitates the exchange of electrons in the intermediate steps of the OER mechanism, thus catalysing the OER kinetics. Electrochemical impedance spectroscopy (EIS) is an effective technique to analyse the reaction properties of an electrode–electrolyte interface. The information regarding the solution resistance (R_s) and charge transfer resistance (R_{ct}), also known as Faraday resistance, at the electrode and electrolyte interface was studied using EIS spectra in the frequency range from 1 kHz to 1 mHz. The EIS spectra of the catalyst were obtained at an OER overpotential of 310 mV and the Nyquist plots of NF and NF/V_2O_5 are shown in Fig. 3(c). The depressed semi-circle indicates that the process follows Butler–Volmer kinetics. NF and NF/V_2O_5 showed charge transfer resistance (R_{ct}) values of 1.86 and 0.53 Ω, respectively, which denote the improved kinetics of the reaction for NF/V_2O_5. To assess the electrochemical surface area (ECSA), the cyclic voltammetry curves were recorded at different scan rates *viz.*, (15, 30, 45, 60, 75, 90, 105, 120, 135, 150, 165, 180 and 195 mV s^{-1}) at the non-faradaic region of 1.1 to

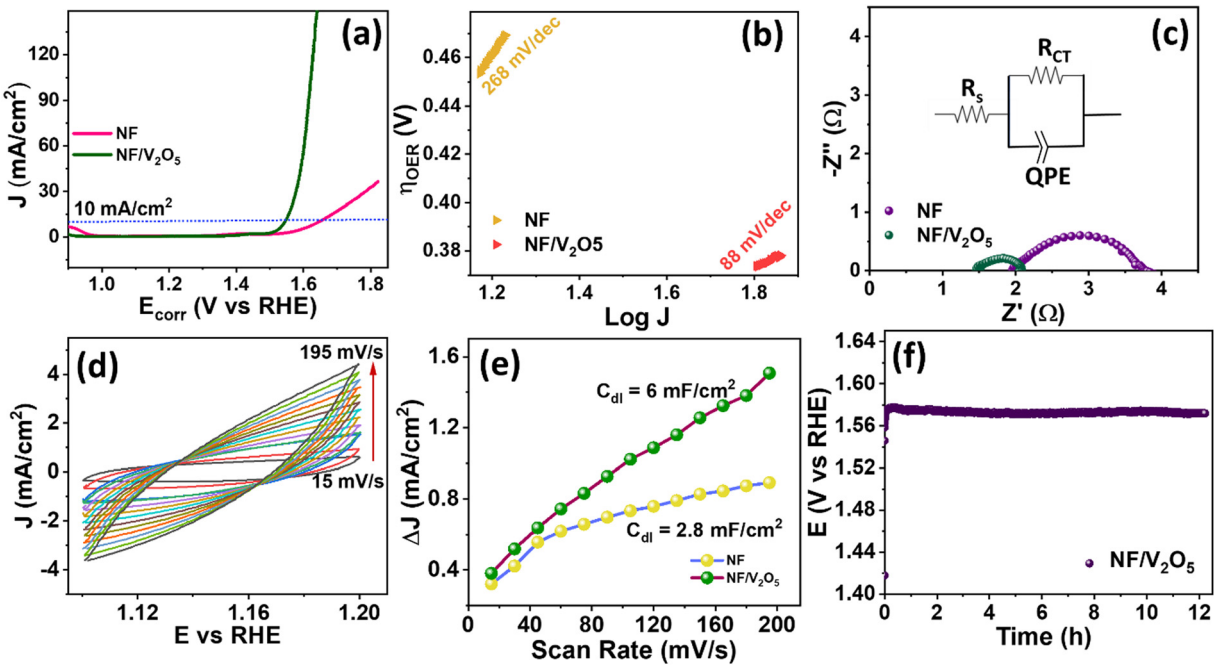

Fig. 3 Electrochemical studies of Ni foam and Ni/V_2O_5 nanorods: (a) LSV profile and (b) Tafel plots, (c) Nyquist plots (inset: cell equivalent circuit), (d) CV plots of Ni/V_2O_5 at different scan rates, (e) EDLC plots to determine C_{dl} and (f) stability analysis of NF/V_2O_5 using chronopotentiometry.

 © 2023 The Author(s). Published by the Royal Society of Chemistry

Open Access Article. Published on 17 April 2023. Downloaded on 10/20/2025 5:22:59 PM.
This article is licensed under a Creative Commons Attribution-NonCommercial 3.0 Unported Licence.

Table 1 Comparison table of VO_x-based materials and their OER performance

Material	Substrate	Tafel slope (mV dec^{-1})	Over potential (mV)	Ref.
$VO(OH)_2/V_2O_5/NiVO_3$	Ni foam	50.1	232	6
VO_x/Ni_3S_2	Ni foam	82	358	7
$MnVO_x$/N-rGO	Carbon fibre paper	66.6	286	8
$Ni_3V_2O_8/FeVO_4$	GCE	52.8	290	9
$Co_3V_2O_8$	Ni foam	20	194	10
$CoOOH/Co_{0.5}(V_{0.5})$	GCE	56	282	11
$CoVO_x$	Ni foam	35	254	12
$N/Co_2V_2O_7$	Ni foam	88	244	13
CoV_2O_6–V_2O_5/N-doped rGO	GCE	49.7	239	14
Co_2VO_4	GCE	54.32	273	15
d-Ti_3C_2MXene/V_2O_5	Ni foam	49	240	16
IrO_2/V_2O_5	GCE	56	266	17
MOF-V_2O_5	Ni foam	50.3	430	18
VO_2	Ni foam	85	150	19
V_2O_5	Ni foam	88	310	This work

1.2 V *vs.* RHE as shown in Fig. 3(d) to determine the double layer capacitance value (C_{dl}). The C_{dl} values obtained from the slopes of the linear plots between scan rate and peak current difference (Fig. 3(e)) yield values of 2.8 mF cm^{-2} for NF and 6 mF cm^{-2} for Ni/V_2O_5. Since C_{dl} is a direct indicator of ECSA (ECSA = C_{dl}/C_s; C_s – specific capacitance, being a constant), it can be understood that the nanorods of V_2O_5 can offer more active sites for reaction with an enhanced ECSA for better catalytic activity. The durability of the NF/V_2O_5 electrocatalyst was studied using chronopotentiometry for delivering a constant current of 5 mA cm^{-2} for 12 h. From Fig. 3(f), it is evident that there is no significant change in the potential for continuous catalysis of 12 h, showing stable operation of V_2O_5 nanorods and their suitability as an efficient electrocatalyst for OER studies. The previous reports of VO_x-based materials used for OER activity studies compared with the present work are shown in Table 1. From the comparison table, it is understood that the present work is the first report on pure V_2O_5 nanorods towards OER studies. Also, it exhibits a comparable result with its counterparts that are doped with various other materials.

Conclusions

A facile polymer-assisted synthesis technique has been adopted in this work to develop polycrystalline V_2O_5 nanorods. XRD and XPS studies helped in analysing the temperature-dependent structural characteristics of the V_2O_5 nanostructures and their oxidation state information. The flat nanorod-like morphology of V_2O_5 gains an advantage by providing more active sites for the catalytic process. This work suggests that the pure V_2O_5 electrocatalyst synthesized in this work provides challenging results in terms of a lower overpotential (310 mV), Tafel slope (88 mV dec^{-1}) and cycling stability over 12 h and can be a promising material for water splitting applications.

Author contributions

Veena Mounasamy: conceptualization, methodology, and writing original draft. Ganesan Srividhya: data curation and formal analysis. Nagamony Ponpandian: validation and supervision.

Conflicts of interest

There are no conflicts to declare.

Acknowledgements

The authors VM, GS and NP would like to express their sincere thanks to Bharathiar University, Coimbatore, Tamil Nadu for providing infrastructure support to carry out the work. One of the authors, VM would like to thank UGC for the Dr D. S. Kothari Post-Doctoral Fellowship (No. F.4-2/2006 (BSR)/PH/20-21/0112 dated 14th September 2021). Authors GS and NP would like to thank TANSCHE for the funding (FILE NO. RGP/2019-20/BU/HECP-0025).

References

1 C. Ji, G. Yang, P. R. Ilango, J. Song, D. Yu, S. Han, D. Zhang, L. Li and S. Peng, *Chem. – Asian J.*, 2020, **15**, 1957–1962.
2 D. Yu, P. R. Ilango, S. Han, M. Ye, Y. Hu, L. Li and S. Peng, *Int. J. Hydrogen Energy*, 2019, **44**, 32054–32065.
3 K. A. Stoerzinger, L. Qiao, M. D. Biegalski and Y. Shao-Horn, *J. Phys. Chem. Lett.*, 2014, **5**, 1636–1641.
4 V. Mounasamy, G. K. Mani and S. Madanagurusamy, *Microchim. Acta*, 2020, **187**, 253.
5 V. Mounasamy, G. K. Mani, D. Ponnusamy, K. Tsuchiya, A. K. Prasad and S. Madanagurusamy, *New J. Chem.*, 2019, **43**, 11069–11081.
6 D. Wang, J. Ru and Y. Hua, *Mater. Lett.*, 2023, **330**, 133340.
7 Y. Niu, W. Li, X. Wu, B. Feng, Y. Yu, W. Hu and C. M. Li, *J. Mater. Chem. A*, 2019, **7**, 10534–10542.
8 X. Xing, R. Liu, K. Cao, U. Kaiser, G. Zhang and C. Streb, *ACS Appl. Mater. Interfaces*, 2018, **10**, 44511–44517.
9 Y. Ma, M. Li, R. Luan, C. Li, X. Liu, H. Zhao, Y. Wang, Y. Chai and B. Dong, *Int. J. Hydrogen Energy*, 2022, **47**, 33352–33360.
10 S. Keerthana, R. Yuvakkumar, G. Ravi, M. Pannipara, A. G. Al-Sehemi and D. Velauthapillai, *ECS J. Solid State Sci. Technol.*, 2021, **10**, 071003.
11 K. Fan, H. Zou, L. Duan and L. Sun, *Adv. Energy Mater.*, 2020, **10**, 1–9.

Open Access Article. Published on 17 April 2023. Downloaded on 10/20/2025 5:22:59 PM.
This article is licensed under a Creative Commons Attribution-NonCommercial 3.0 Unported Licence.

12 L. Liardet and X. Hu, *ACS Catal.*, 2018, **8**, 644–650.
13 Z. Luo, Q. Peng, Z. Huang, L. Wang, Y. Yang, J. Dong, T. T. Isimjan and X. Yang, *J. Colloid Interface Sci.*, 2023, **629**, 111–120.
14 F. C. Shen, Y. Wang, Y. J. Tang, S. L. Li, Y. R. Wang, L. Z. Dong, Y. F. Li, Y. Xu and Y. Q. Lan, *ACS Energy Lett.*, 2017, **2**, 1327–1333.
15 M. K. Sahoo, N. Bishoyi, D. K. Swain and J. N. Behera, *Sustainable Energy Fuels*, 2022, 4779–4786.
16 I. Ashraf, S. Ahmad, F. Nazir, D. Dastan, Z. Shi, H. Garmestani and M. Iqbal, *Int. J. Hydrogen Energy*, 2022, **47**, 27383–27396.
17 X. Zheng, M. Qin, S. Ma, Y. Chen, H. Ning, R. Yang, S. Mao and Y. Wang, *Adv. Sci.*, 2022, **9**, 2104636.
18 S. Ji, A. Muthurasu, K. Chhetri and H. Yong, *J. Colloid Interface Sci.*, 2022, **618**, 475–482.
19 T. V. M. Sreekanth, M. Tamilselvan, K. Yoo and J. Kim, *Appl. Surf. Sci.*, 2021, **570**, 151119.

 © 2023 The Author(s). Published by the Royal Society of Chemistry